Australian Journal of Basic and Applied Sciences, 7(10): 332-339, 2013
ISSN 1991-8178

Advantages of Integration Molten Salt Cavity Tubular Solar Central Receiver to the Boiler of Existing Gas-Fuelled Conventional Steam Power

[1,2]Mahmood S. Jamel, [2]A. Abd Rahman, [2]A.H. Shamsuddin

[1]Mechanical Engineering Dept., College of Engineering, University of Basrah, Basrah, Iraq
[2]Centre for Renewable Energy, Universiti Tenaga Nasional, 43000, Kajang, Selangor, Malaysia

Abstract: This paper introduces a new method to integrate the economizer of the AL-Hartha steam plant located in Basra, Iraq, using a molten salt cavity tubular solar central receiver (SCR). Cycle Tempo is used to simulate the existing natural gas-fuelled conventional steam power cycle with consideration of the heat and pressure losses. The heliostat field and the central receiver subsystems are coded using MATLAB. The model couples the heat balance with the temperature computation of the receiver walls for calculation and analysis of the thermal losses. The proposed modified codes are capable of calculating heat losses, evaluating the integrated power plant and satisfying a wide range of SCRs. The results are verified against plant data and previous works in the literature and good agreement is obtained. The results show the potential of using a molten salt cavity tubular SCR for low-range temperature in boiling process in the plant boiler, the economizer part. It is observed that the obtained receiver energy efficiency can reaches up to 94.1% and the maximum reduction in instantaneous gas fuel consumption is about 9.1% .

Key words: hybrid power plants, solar electric generating system, solar aided power generation, feedwater preheating, economizer.

INTRODUCTION

With the pressure of global warming and the increase in oil prices, the application of solar energy is getting more and more attention. It is a free and non-depleting energy source with no carbon emissions. Many negative factors such as its relatively low intensity, the change of weather and seasons, etc., make the application of the solar energy inefficient, unsteady, costly, limiting its further applications. An attractive option using solar thermal to integrate existing steam plants become reality in the last decades and should be takes as road map for clean energy in near future.The early work to use solar thermal with existing steam plant started in 1975 with Zoschak and Wu (Zoschak and Wu 1975) by studying seven methods of absorbing solar energy as the direct thermal input to an 800 MW fossil-fuelled central station steam power plant. Their results showed the combined evaporation and superheating to be the preferred method for hybridization. Odeh (Odeh 2003) analyzed utilizing the solar energy in boiling process arrangement, preheating process arrangement, preheating and boiling process arrangement, he observed that the boiling process arrangement is the most conducive to reduce fossil fuel. Many studies have focused on using solar-aided power generation (SAPG) to replace part of the extraction steam(Ying and Hu 1999, Pai 1991, Gupta and Kaushik 2010, Hu *et al*. 2010, Suresh, Reddy and Kolar 2010, Popov 2011, Yang *et al*. 2011, Jamel, Abd Rahman and Shamsuddin 2013) and a little on boiling process in boiler.

Jun Z (Jun 2011) analyzed two types of integration arrangements on the basis of direct steam generation: the arrangement before economizer and the arrangement after economizer. his results indicated that with the same direct solar radiation and solar collector area the coal and spraywater consumption is reduced due to the solar energy which replaces part of the coal supply to the boiler system under the condition of maintaining a constant rated evaporation capacity, and the arrangement before economizer has more coal reductions and less spraywater reductions than the arrangement after economizer, and the arrangement after economizer has better system stability in steam production than the arrangement before economizer. There is a little research has been done to examine boiling process arrangement for utilizing solar energy in gas fuelled power plants. This paper tried to do such analysis using molten salt cavity tubular solar central receiver as solar thermal system(STS) .

Computational Methodology:

Modelling of Existing Steam Cycle :

The selected case study is the AL-Hartha steam power plant located in Basra, Iraq. The superheated steam enters the two-stage single reheat steam turbine at 541 °C/125 bar and 541 °C/36.77 bar, for the high- and

Corresponding Authors: Mahmood S Jamel, Mechanical Engineering Dept., College of Engineering, University of Basrah, Basrah, Iraq.
E-mail: mahmood_shaker2005@yahoo.co.uk

intermediate-pressure stages, respectively. Steam enters the low-pressure stage with a pressure of 6.934 bar; the condenser pressure is 80 kPa. The simulation process done using Cycle-Tempo as shown in Fig.1.

Modelling of Heliostat Field Subsystem:

A simple model is implemented to determine the solar position described in (Chong and Tan 2011). The overall field efficiency η_{field} is expressed by the following equation:

$$\eta_{field} = \eta_{cos} x\eta_{atten} x\eta_{Blok\ \&shadow} x\eta_{reft} x\eta_{spill}$$

The cosine efficiency of a heliostat is equal to the cosine of incidence angle θ relative to the heliostat centre and is given by $\eta_{cos} = \cos\theta$. The atmospheric attenuation efficiency can be calculated simply as a function of the distance between the heliostat and the receiver in metres (Schmitz *et al*. 2006):

$$\eta_{atten} = 0.99321 - 0.001176S + 1.97x10^{-8}S^2 \qquad S \leq 1000m$$

$$\eta_{atten} = e^{-0.0001106\,S} \qquad S < 1000m$$

where S is the distance between the heliostat and the receiver. The actual mirror reflectivity is taken as $\eta_{reft} = 0.836$. The consideration of the heliostats never overlapping is considered here; thus the shading and blocking losses are equal zero or $\eta_{Blok\ \&shadow} = 1$. In addition, because the scope of the present study considers only the total area generated, there is no need to describe the field layout and therefore, there no need to include minor losses; thus, η_{spill} =1. The incident solar radiation Q_{solar} is proportional to the total area of the heliostat field and can be expressed as the product of the direct normal irradiance for the surface hit by the sunlight:

$$Q_{solar} = DNI.A_{field}$$

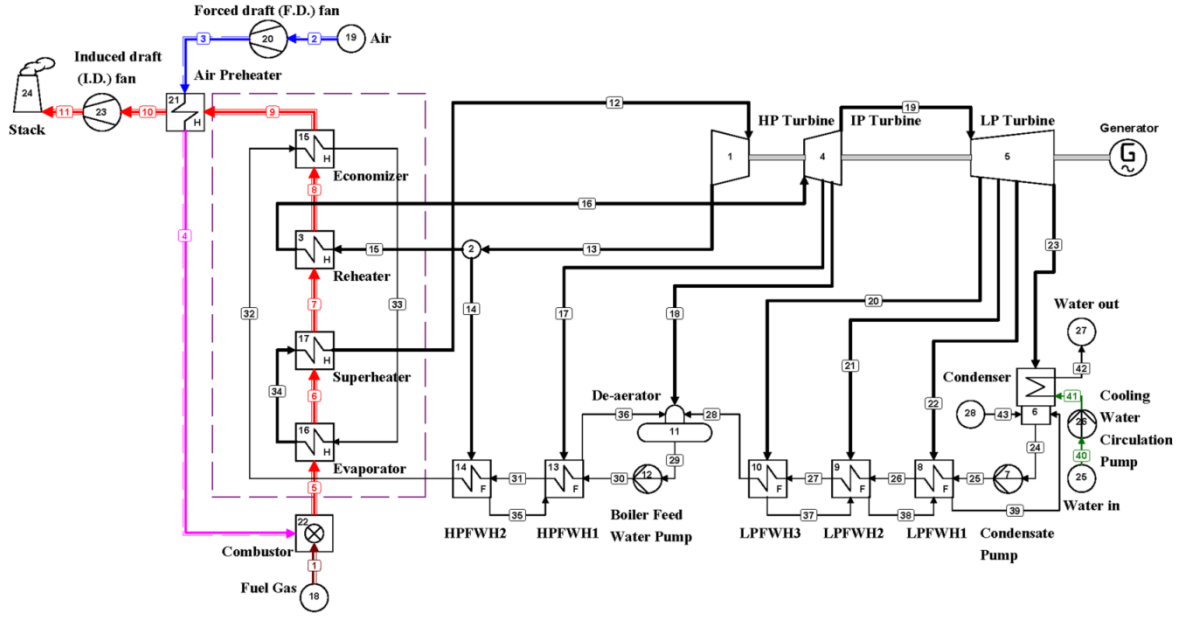

Fig. 1: Schematic diagram for existing 200 MW unit at AL-Hartha Steam power plant.

The incident power into the receiver aperture from the heliostat field (power to the receiver) $Q_{rec,}$ is calculated by (Yao *et al*. 2009):

$$Q_{rec} = DNI.A_{field}.\eta_{field}.\Gamma$$

The exergy E_{solar} associated with the solar irradiation on the heliostat mirror surface Q_{solar} can be expressed as:

$$E_{solar} = Q_{solar}\,(1 - T_a/T_s)$$

where T_S is the apparent sun temperature as an exergy source and taken to be 4500 K (Xu *et al*. 2011). Similarly, the exergy delivered to the receiver is written as:

$$E_{rec} = Q_{rec}\,(1 - T_a/T_s)$$

Energy losses for the heliostat field are:

$$Q_{loss.H} = Q_{Solar} - Q_{rec}$$

The exergy losses for the heliostat field IR_H are:

$$IR_H = E_{solar} - E_{rec}$$

The energy efficiency and exergy efficiency of the heliostat field subsystem are given by:

$$\eta_{I.H} = \frac{Q_{rec}}{Q_{solar}}$$

$$\eta_{II.H} = \frac{E_{rec}}{E_{solar}}$$

Modeling of The Central Receiver Subsystem:

The purpose of the current study is the integration of CSR to an existing steam plant. With such technologies and as the limitations of the design and working conditions for these existing plants and becoming older, there is no need to use advanced technology and higher temperatures provided by volumetric receivers. In addition, the latter are an underdeveloped technology and the superheated steam receiver has poor steam heat-transfer capabilities (Kribus, Ries and Spirkl 1996, Buck *et al*. 2006). Among the available types of CSRs, a cavity tubular receiver with molten salt as the working fluid was selected as offering the potential to be one of the most cost effective and safe receivers. This type of receiver is divided into two parts: stainless steel tubes and flowing molten salt in tubes. The analysis here is based on the cavity receiver. In operation, the receiver absorbs the insolation Q_{rec} and transports part of the energy to the molten salt flowing through it. The remainder of the energy is lost to the environment by convective, emissive, reflective and conductive heat losses and is expressed by the receiver total heat loss $Q_{rec.totloss}$. The energy balance and exergy balance for the central receiver are:

$$Q_{rec} = Q_{rec.abs} + Q_{rec.totloss}$$

$$E_{rec} = E_{rec.abs} + E_{rec.totloss} + IR_{rec}$$

where $Q_{rec.abs}$ is the receiver absorbed heat, this parameter is taken as design point for receiver and calculated by

$$Q_{rec.abs} = \dot{m}_{water}\,\Delta h = \dot{m}_{ms}\,Cp_{ms}\,(T_{ms.out} - T_{ms.in})$$

It's important to mention here that the molten salt temperatures is compatible with temperature difference for integrated part. The exergy loss associated with the heat loss is expressed as:

$$E_{rec.totloss} = Q_{rec.totloss}\,(1 - T_a/T_{rec.sur})$$

While The useful exergy absorbed by flowing heat transfer fluid are expressed by:

$$E_{rec.abs} = \dot{m}_{ms}\,Cp_{ms}\,[(T_{ms.out} - T_{ms.in}) - T_a\,\ln(T_{ms.out}/T_{ms.in})]$$

Then, the energy efficiency and exergy efficiency of the central receiver subsystem are defined as

$$\eta_{I,rec} = \frac{Q_{rec.abs}}{Q_{rec}}$$

$$\eta_{II,rec} = \frac{E_{rec.abs}}{E_{rec}}$$

A modified thermal model for the molten salt cavity receiver is used here to calculated total heat losses, the detail model and parameters can reviewed in reference (Li *et al*. 2010):

$$Q_{rec.totloss} = Q_{rec.conv} + Q_{rec.em} + Q_{rec.ref} + Q_{rec.con}$$

Table 1: Properties of the base case solar tower power plant.

Subsystem	Properties	Values Unit
Heliostat field	Beam radiation (DNI)	850 Wm^{-2}
	The latitude	30.677°
	The longitude	47.816°
	Day number	196
	The distance between the heliostat and the receiver	1000m
	The radial distance between heliostat and	55m
	The height of the heliostat	7m
	The target height	95m
	The facing angle	63°
	Local time	14 hour
Central receiver	Aperture area	16.96 m^2
	Inlet temperature of molten salt	290 °C
	Outlet temperature of molten salt	560 °C
	View factor	0.8
	Tube diameter	0.019 m
	Tube thickness	0.00165 m
	Emissivity	0.8
	Aperture height	6 m
	Reflectivity	0.04
	Conductivity of tube material	19.7 W/mK
	Conductivity of insulation	40 W/mK
	Insulation layer thickness	0.07
	Wind velocity	5.0 m/s

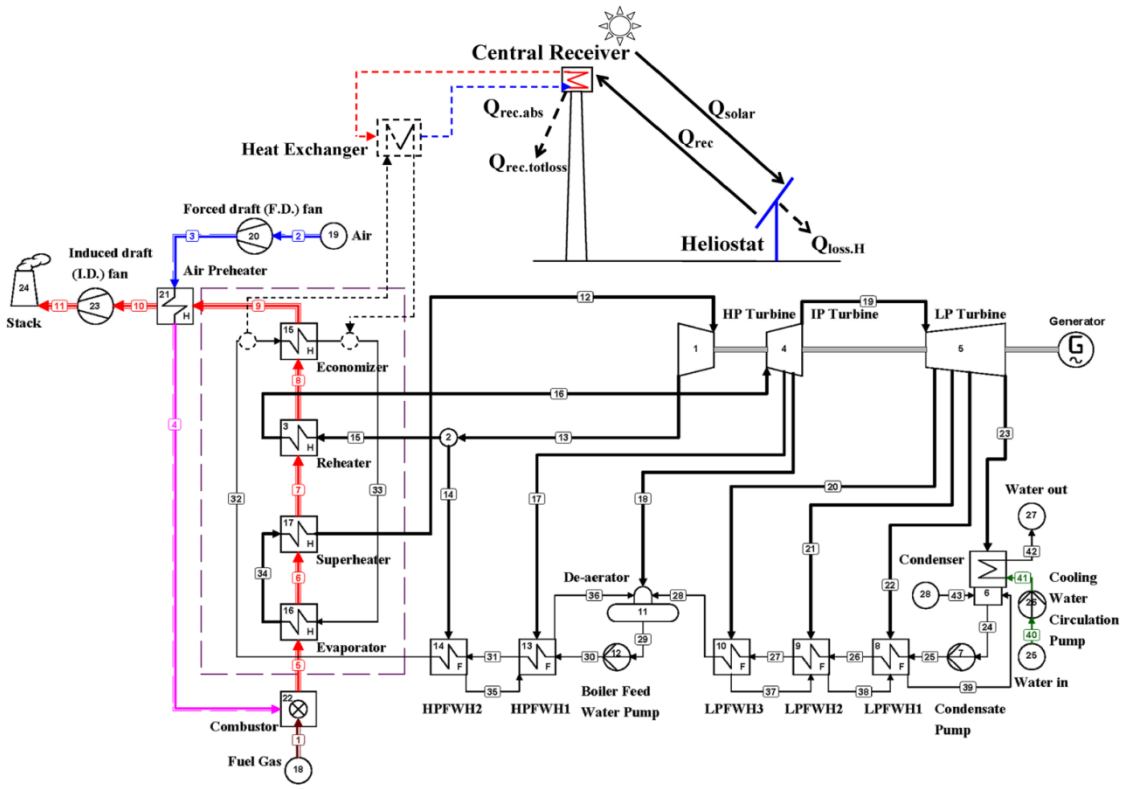

Fig. 2: Schematic representation integration of Economizer with molten salt cavity tubular solar central receiver.

RESULTS AND DISCUSSION

Results Validation:

The evaluation criteria to suggested plant modification in the present analysis is based on the energy balance and exergy balance of each subsystem. simulation other operating units that exactly similar to the damaged units using Cycle Tempo for full load operation as shown in Figure 1, This simulated cycle is verified with practical data collected from the actual plant and good results are obtained. The analysis for the central receiver is based on a thermal model, which is modified from a validated model developed by Li *et al*(Li *et al*. 2010) and C. Xu *et al*. (Xu *et al*. 2011). To validate the modification, the present model was used to calculate the thermal performance of the Sandia National Laboratories' molten salt electric experiment(MSEE) based on

the parameters provided in ref. (Li *et al*. 2010). The calculated energy efficiency of the receiver is 86.66%, which gives acceptable agreement with ref (Xu *et al*. 2011, Li *et al*. 2010). While for heliostat field subsystem, the calculated efficiencies agree the results shown in ref (Yao *et al*. 2009) therefore the paper results are reasonable and useful for guiding the design and integration of CSR.

Results Discussion:

The paper discussed the impact of economizer integration with molten salt cavity tubular solar central receiver with a temperature range from 242 to 297°C on the existing gas-fueled fired power plant. These temperatures range used as design point for central receiver, its mean not used fixed temperatures range that used in previous works. The feed water from heaters is received by the boiler, going through the economizer first, The integration scheme proposed enters the water to additional heat exchanger that put in parallel with the fired economizer in order to receive the heat from molten salt instead flue gas, and then the hot water goes to the next part of the boiler that is evaporator as showing in Fig. 2 . Such integration allow for hybrid or stand alone operation but needing to add some heat exchangers and modify piping system. The CSR model in compatible with Cycle Tempo was run in thermodynamic and engineering design mode to evaluate performance, calculate solar field capacity and basic configuration. The selected operation mode for such integration is fuel conservation mode in which the gross power output keep constant or constant rated evaporation capacity. The effect of such integration on the plant energy and exergy bases in fuel conservation mode were discussed and evaluated.

The heat from the SCR has an effect on the performance of the boiler. The rated evaporation capacity keeping constant during operation in order to stable plant operation. Table 2 shows the stream data for the plant as existing and after integrated SCR. It's clear the flow rates of water-steam cycle keep constant after integration while see some decrease in fuel consumption that account the amount of heat absorbed by economizer as shown in Figure 3. According to the calculation results of the integration, there is 9.1% reduction in gas fuel consumption due to the integration of the solar energy into the boiler system that achieving the targets of energy saving. For the integrated CSR, there are some attractive results. The main result is the ability of integration of CSR for proposed range of temperatures. CSR divided here into two subsystems that are heliostats field and central receiver for details evaluation purpose. The effect of such integration as well as the change of performance parameters are shown in Table 3. In general, the energy and exergy efficiencies for existing and integrated plant are same as the consideration of constant rate of evaporation kept the net power deliver has very slightly increasing that not effected the plant efficiencies. For the heliostat field, the field energy and exergy efficiencies are constant at 63.8% , as its related to the selected site, date, time and other technical input that shown in Table 1. Also, there is about 91325.3m^2 of heliostat field required to cover this modification. The receiver energy efficiency reaches high values to about 95.3% as the high values of solar absorbed heat $Q_{rec.abs}$.

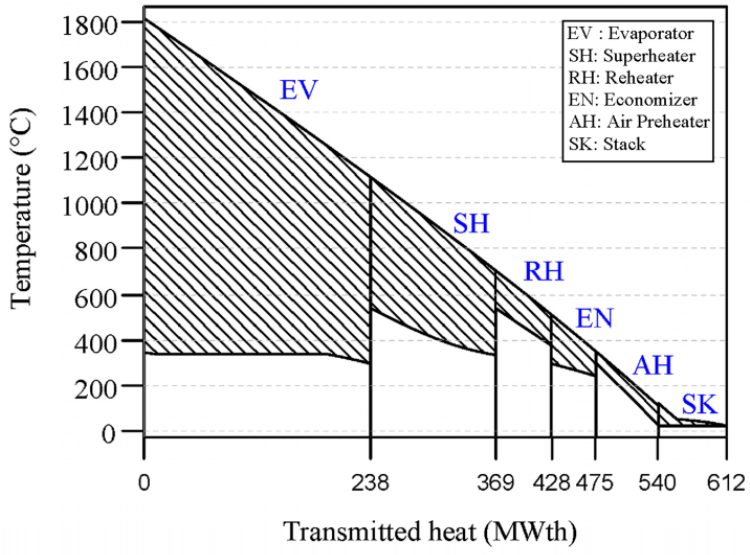

Fig. 3: The amount of heat transmitted for each part of boiler.

Table 2: Stream data for existing and integrated gas fueled fired power plant.

Outlet Pipe as Fig.2	Mass flow (kg/s)	Pressure (bar)	Temperature (°C)	Total Energy flow (MW_{th})	Total Exergy flow (MW_{th})
Natural gas					
1	10.9 (9.9)	1.031	25	556.2 (551.9)	523.4 (519.3)
Air/Flue gases					
2	236.2 (234.4)	1.013	25	3.9 (3.8)	0.2 (0.2)
3	236.2 (234.4)	1.036	27.7	4.5 (4.5)	0.6 (0.6)
4	236.2 (234.4)	1.031	300	70.5 (70.0)	20.2 (20.0)
5	247.2 (244.3)	1.031	1811.8	62.7 (62.2)	407.7 (404.5)
6	247.2 (244.3)	1.011	1115.3 (1176.6)	407.5 (384.1)	225.1 (207.3)
7	247.2 (244.3)	1.001	705.8 (806.7)	286.6 (252.9)	132.6 (109.2)
8	247.2 (244.3)	1.000	512.8 (614.4)	226.6 (194.4)	90.5 (70.3)
9	247.2 (244.3)	0.980	350	148.4 (147.3)	43.1 (42.8)
10	247.2 (244.3)	0.971	112.6	82.4 (81.7)	16.5 (16.3)
11	247.2 (244.3)	1.060	124.1	85.5 (84.8)	19.1 (18.9)
Water/Steam					
12	173.7	124.8	538.3	581.4	259.0
13	173.7	38.7	379.5	532.9	204.5
14	17.9	36.8	377.8	54.9	20.9
15	155.8	36.8	377.8	478.0	182.4
16	155.8	34.9	540.2	536.5	215.9
17	7.1	14.7	420.2	22.6	7.9
18	6.2	6.7	318.5	18.7	5.6
19	142.5	6.9	315.6	426.4	129.6
20	6.3	3.2	235.4	18.0	4.6
21	7.0	1.4	156.1	18.8	3.9
22	8.6	0.48	80.2	21.8	3.3
23	120.4	0.090	43.8	280.7	17.2
24	142.5	0.080	41.5	11.7	0.3
25	142.5	6.8	43.8	11.8	0.4
26	142.5	6.8	77.2	31.7	2.6
27	142.5	6.7	107.0	49.6	5.9
28	142.5	6.7	133.0	65.3	9.8
29	173.7	6.7	163.6	102.6	18.6
30	173.7	154	166.0	105.9	21.6
31	173.7	146.8	194.4	127.3	28.9
32	173.7	146.7	242.4	165.0	43.8
33	173.7	145.1	296.9	212.2	65.2
34	173.7	131.4	340.4	450.1	185.5
35	17.9	14.71	197.3	17.2	4.3
36	24.9	6.766	163.5	18.4	3.8
37	6.3	1.436	110.0	2.3	0.3
38	13.3	0.478	80.2	3.2	0.2
39	22.0	0.090	43.8	5.1	0.2
40	8201.6	1.013	25	34.3	0
41	8201.6	1.27	25	34.5	0.2
42	8201.6	1.07	33	308.7	4.6

Values in parentheses refer to integrated plant with CSR

Table 3: Effect of performance factors on the existing plant.

Subsystem	Performance parameter	schemes	
		A	B
Existing gas fuel steam cycle	Net absorbed energy (MW_{th})	500.5	500.4
	Net unit capacity (MW)	187.1	187.5
	Net energy efficiency (%)	37.4	37.4
	Net exergy efficiency (%)	36.1	36.1
The Heliostat field subsystem	The incident solar radiation(MW_{th})	0	77.6
	The exergy associated with the solar irradiation (MW_{th})	0	72.5
	Heliostat field heat losses; (MW_{th})	0	28.1
	Exergy losses for the heliostat field (MW_{th})	0	2.6
	The energy efficiency of the heliostat field (%)	0	63.8
	The exergy efficiency of the heliostat field (%)	0	63.8
	The area of heliostat field (m^2)	0	91325.3
The Receiver Subsystem	The incident power into receiver aperture from the heliostat field (MW_{th})	0	49.6
	The Receiver total heat loss (MW_{th})	0	2.3
	The exergy delivered to the receiver (kW_{th})	0	46.3
	The exergy loss associated with the heat loss(MW_{th})	0	1.4
	The exergy losses for the central receiver (MW_{th})	0	27
	The energy efficiency of the receiver (%)	0	95.3
	The exergy efficiency of the receiver (%)	0	63.5
The Integrated	Natural gas consumption (kg/s)	10.9	9.9
cycle	Natural gas conservation (%)	0	9.1

Conclusions:

The integration of the AL-Hartha steam plants economizer with a molten salt cavity tubular SCR are proposed in this paper. This integration is evaluated through a modified model for both the existing power plant and the integrated SCR in order to determine the best solution offering the highest performance. The using of a molten salt cavity tubular SCR for low-range temperature in first part of boiling process was verified. The SCR that offers the highest performance was also investigated. The energy efficiency of the receiver reaches up to 95.3% and the maximum reduction in instantaneous gas fuel consumption is about 9.1%.

ACKNOWLEDGMENTS

The authors would like to thank the Energy Technology Section, Delft University of Technology, The Netherlands for licensing a copy of Cycle-Tempo and Mr. Mark Roest for providing technical support. Also, thanks go to the staff of AL-Hartha steam plant for their efforts in providing plant technical data.

Abbreviation

A	Area(m^2)
STS	solar thermal system
d	diameter (m)
DNI	Direct Normal Irradiance
SAPG	solar aided power generation

Nomenclature

SCR	Solar Central Receiver
Cp	specific heat at constant pressure ($W/m^2.K$)
F_r	View factor
h	heat transfer coefficient($W/m^2.K$)
k	Conductivity (W/m.K)
Q	heat (kW)
m	mass flow rate(kg/s)
T	temperature (°C)
S	distance from the heliostat and the receiver(m)

Greek symbol

ε	emissivity
Γ	the fraction of the field in track
η	efficiency
σ	Stefan–Boltzmann constant $5.67x10^{-8}$ ($W/m^2.K^4$)

Subscript

a	ambient
abs	absorbed energy
air	air
avg	average
con	conductive heat loss
conv	convective heat loss
em	emissive heat loss
fc	forced convection
i	inner tube or inlet
insu	insulation
isni	inner side of receiver
loss	heat loss
ms	molten salt
nc	natural convection
o	outer tube or outlet
rec	receiver
ref	reflective heat loss
s	solar
sur	surface
totloss	total heat loss
tube	receiver absorber tube
w	wall surface

REFERENCES

Buck, R., C. Barth, M. Eck, W.D. Steinmann, 2006. Dual-receiver concept for solar towers. *Solar Energy*, 80: 1249-1254.

Chong, K.K., M.H. Tan, 2011. Range of motion study for two different sun-tracking methods in the application of heliostat field. *Solar Energy*, 85: 1837-1850.

Gupta, M.K., S.C. Kaushik, 2010. Exergy analysis and investigation for various feed water heaters of direct steam generation solar–thermal power plant. *Renewable Energy*, 35: 1228-1235.

Hu, E., Y. Yang, A. Nishimura, F. Yilmaz, A. Kouzani, 2010. Solar thermal aided power generation. *Applied Energy*, 87: 2881-2885.

Jamel, M.S., A. Abd Rahman, A.H. Shamsuddin, 2013. Advances in the integration of solar thermal energy with conventional and non-conventional power plants. *Renewable and Sustainable Energy Reviews*, 20: 71-81.

Jun, Z., 2011. Analysis of Solar Aided Steam Production in a Pulverized Coal Boiler. In *Power and Energy Engineering Conference (APPEEC), 2011 Asia-Pacific*, 1-4.

Kribus, A., H. Ries, W. Spirkl, 1996. Inherent Limitations of Volumetric Solar Receivers. *Journal of Solar Energy Engineering*, 118: 151-155.

Li, X., W. Kong, Z. Wang, C. Chang, F. Bai, 2010. Thermal model and thermodynamic performance of molten salt cavity receiver. *Renewable Energy*, 35: 981-988.

Odeh, S.D., 2003. Unified model of solar thermal electric generation systems. *Renewable Energy*, 28: 755-767.

Pai, B.R., 1991. Augmentation of thermal power stations with solar energy. *Sadhana*, 16: 59-74.

Popov, D., 2011. An option for solar thermal repowering of fossil fuel fired power plants. *Solar Energy*, 85: 344-349.

Schmitz, M., P. Schwarzbözl, R. Buck, R. Pitz-Paal, 2006. Assessment of the potential improvement due to multiple apertures in central receiver systems with secondary concentrators. *Solar Energy*, 80: 111-120.

Suresh, M.V.J.J., K.S. Reddy, A.K. Kolar, 2010. 4-E (Energy, Exergy, Environment, and Economic) analysis of solar thermal aided coal-fired power plants. *Energy for Sustainable Development*, 14: 267-279.

Xu, C., Z. Wang, X. Li, F. Sun, 2011. Energy and exergy analysis of solar power tower plants. *Applied Thermal Engineering*, 31: 3904-3913.

Yang, Y., Q. Yan, R. Zhai, A. Kouzani, E. Hu, 2011. An efficient way to use medium-or-low temperature solar heat for power generation – integration into conventional power plant. *Applied Thermal Engineering*, 31: 157-162.

Yao, Z., Z. Wang, Z. Lu, X. Wei, 2009. Modeling and simulation of the pioneer 1MW solar thermal central receiver system in China. *Renewable Energy*, 34: 2437-2446.

Ying, Y., E.J. Hu, 1999. Thermodynamic advantages of using solar energy in the regenerative Rankine power plant. *Applied Thermal Engineering*, 19: 1173-1180.

Zoschak, R.J., S.F. Wu, 1975. Studies of the direct input of solar energy to a fossil-fueled central station steam power plant. *Solar Energy*, 17: 297-305.